Surface Characterization and Functionalization of MCM-41 Silicas via Silazane Silylation

Reiner Anwander,* Iris Nagl, and Markus Widenmeyer

Anorganisch-chemisches Institut der Technischen Universität München, Lichtenbergstrasse 4, D-85747 Garching, Germany

Günter Engelhardt, Olaf Groeger, Clemens Palm, and Thomas Röser

Institut für Technische Chemie, Universität Stuttgart, D-70550 Stuttgart, Germany

Received: September 1, 1999; In Final Form: January 20, 2000

Disilazane reagents of type $HN(SiR^1R^2_2)_2$ carrying organic substituents $R^{1,2}$ = H, Me, Ph, *n*-Bu, *n*-Oct, Vin (Vin = vinyl) of varying longitudinal and lateral extension are reacted with high quality MCM-41 samples of different pore sizes, i.e., effective pore diameters of 2.8 and 3.8 nm according to the BJH pore size analysis of the desorption branch. The reaction of the standard silylating reagent hexamethyldisilazane, $HN(SiMe_3)_2$, is shown to be controlled by the amount of added silylamine and the contact time, resulting in effective pore size engineering. Calculations from elemental analysis revealed that the degree of silylation (silylation efficiency) and hence the surface hydroxyl consumption depend on the steric bulk/shape of the groups R. The surface coverage varies from 0.74 to 1.85 silyl groups/nm^2. The sterically least demanding tetramethyldisilazane, $HN(SiHMe_2)_2$, is the most efficient silylating reagent, while silyl groups with bulky phenyl substituents produce the lowest surface coverage featuring considerable interaction with nonsilylated silanol groups. The formation of various covalently linked siloxy functionalities $[OSiR^1R^2_2]$ is reflected in the change of the pore volume and mean pore diameter as evidenced by nitrogen physisorption measurements at 77.4 K. A monofunctional surface reaction and the structural integrity of the immobilized (functionalized) silyl groups is quantitatively revealed by means of FT IR and $^1H/^{13}C$ MAS NMR spectroscopy. Heterobisilylated organic/inorganic hybrid materials are synthesized both via *consecutive* and *competitive* silylation utilizing mixtures of silylamines. The latter silylation procedure provides important mechanistic and kinetic details of this peculiar surface silylation reaction emphasizing the preformation of a four-centered "O···H···N···Si" transposition as the rate-determining step. Fully silylated materials carrying reactive vinyl moieties were functionalized by hydroboration with BH_3(THF) and 9-BBN.

Introduction

Mesoporous oxides such as the structurally ordered and thermally robust silica MCM-41 are classified as promising support materials for the immobilization of catalytically relevant species or as highly efficient adsorbents.[1] For catalytic applications, fine-tuning of the catalytically active interface via adjustment of both the number and accessibility of the catalytically active sites by steric and hydrophobicity effects is known to be crucial.[2] Post-synthetic modification of structurally highly ordered MCM-41 materials[3] offers an alternative route compared to the co-condensation "one-pot" reactions of differently functionalized silanes in the presence of a templating reagent.[4] Silylation reactions are of fundamental importance for the manipulation of siliceous support materials including zeolites.[5,6] Silylating reagents such as chlorosilanes, alkoxysilanes, and silylamines have found widespread application, and their reaction with surface silanol functionalities has been reported in detail (Scheme 1).[7−9]

As a rule chlorosilanes, $SiCl_xR_{(4-x)}$ (Scheme 1, (1)), and alkoxysilanes, $Si(OR)_xR_{(4-x)}$ (Scheme 1, (2)), require more drastic reaction conditions, i.e., the reaction takes place at

SCHEME 1. Methods of Surface Silylation. Pool of Disilazane Reagents Employed for This Study

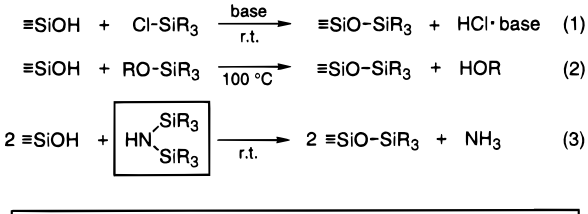

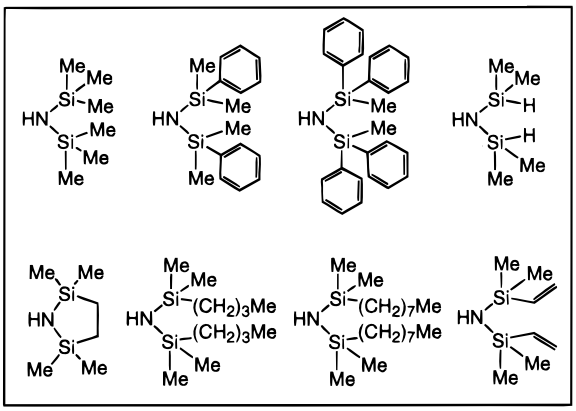

* Corresponding author. Fax: +49 89 289 13473. E-mail: reiner.anwander@ch.tum.de.

10.1021/jp993108d CCC: $19.00
Published on Web 03/23/2000

elevated temperature and in the presence of catalytic (e.g., H_2O) or stoichiometric amounts of additives (e.g., pyridine). In addition, these silylating reagents often display multifunctional surface reactions producing (undesired) byproducts such as alcohols and alkylammonium halides which are difficult to separate. In contrast, silazane-based silylation reactions are characterized by (i) mild reaction conditions, (ii) a relatively slow surface reaction, (iii) a monofunctional surface reaction, (iv) favorable atom economy, and (v) ease of thermal desorption of the byproduct ammonia (Scheme 1, (3)).[10] Given these unique reactivity patterns and the pool of (functionalized) silylamines which is commercially available and synthetically readily accessible (selected examples employed in this study are depicted in Scheme 1), we recently started liquid phase disilazane derivatization reactions of mesoporous silicas in order to exploit their potential as structural probes and to tailor the oxidic support for catalytic applications.[11] Here we report on various options of disilazane silylation and give a full account on the synthesis and physicochemical characterization (MAS NMR spectroscopy, nitrogen physisorption) of such post-silylated MCM-41 materials.

Experimental Section

Synthesis. *Materials*. Sodium water glass (Merck, 28.5 wt.-% SiO_2, 8.5 wt.-% Na_2O, rest water) was used as the silica source for the purely siliceous MCM-41 materials. The surfactant reagent $[C_{16}H_{33}N(CH_3)_3]Br$, hexadecyltrimethylammonium bromide (C_{16}TMABr), was purchased from Aldrich. *n*-Hexane and tetrahydrofuran (THF) were distilled from Na/K/benzophenone. 1,1,1,3,3,3-Hexamethyldisilazane and 1,1,3,3-tetramethyldisilazane were obtained from Aldrich. 1,3-Di-*n*-butyltetramethyldisilazane was purchased from Lancester. Other disilazane reagents (1,3-diphenyltetramethyldisilazane, 1,1,3,3-tetraphenyldimethyldisilazane, 1,3-divinyltetramethyldisilazane, 2,2,5,5-tetramethyl-2,5-disila-1-azacyclopentane, 1,3-di-*n*-octyltetramethyldisilazane) were acquired from GELEST. All of the disilazane reagents were degassed (freeze−pump−thaw if a liquid) prior to use. The borane reagents BH_3(THF) (1 M in THF) and 9-BBN (9-borabicyclo-[3.3.1]nonane, 0.5 M in THF) were used as received from Aldrich. All of the silylated and borylated materials were synthesized from the dehydrated MCM-41 materials and manipulated with rigorous exclusion of air and water, using high-vacuum and glovebox techniques (MB Braun MB150B−G-II; O_2 < 1 ppm, H_2O < 1 ppm).

*Synthesis of MCM-41 Materials **1** and **2** with Different Pore Sizes*. According to established literature procedures,[12,13] the reproducibility of the hydrothermal syntheses could be enhanced by the utilization of various gel additives. Stabilization of the pH value of 11 during the hydrothermal synthesis of **1** was achieved by final addition of glycine as a buffer. Adjustment of the pH value during hydrothermal synthesis was recently shown to be important for the isolation of high-quality, i.e., structurally highly ordered, MCM-41 materials.[14] The quality and reproducibility of the mesitylene-expanded[12,15] material **2** could be significantly increased by addition of excess of sodium chloride prior to hydrothermal treatment. The decreased solubility of mesitylene in NaCl solutions seems to prevent the organic additive from leaching from the unpolar part of the micellar template arrangement. Improvement of the thermal stability of MCM-41 silicas by similar salt effects has been reported previously in the case of mesitylene-free synthesis gels.[16] After calcination (N_2: 540 °C, 5 h, heating rate 1.5 °C min^{-1}; air: 540 °C, 5 h) and dehydration (280 °C, 10^{-5} Torr, 4 h, heating rate 1 °C min^{-1}), the parent materials were characterized by FTIR spectroscopy, powder X-ray diffraction (Figure 1), and nitrogen physisorption at 77.4 K (Table 1, Figure 2) and stored in a glovebox. As the total number of OH groups per nm^2 is a function of the pretreatment temperature, all MCM-41 materials were dehydrated at the same temperature. We found that thermal treatment above 300 °C and $<10^{-4}$ Torr led to a partial collapse of the mesopore structure as revealed by nitrogen physisorption.

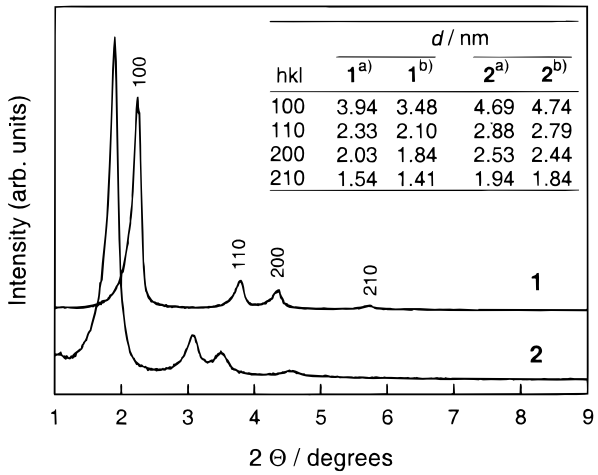

Figure 1. Powder diffraction patterns of as-synthesized materials **1** and **2**; hexagonal lattice parameters of the (a) as-synthesized and (b) calcined form.

The powder X-ray diffractogram of the mesitylene-expanded material **2** reveals a considerable shift of the characteristic low-angle four-peak pattern to lower Θ angles in comparison to material **1**. The thickness of the pore walls of the calcined materials **1** and **2** are derived as approximately 1.2 nm (**1**) and 1.7 nm (**2**), respectively, from the length of the crystallographic *a* axes ($a = d_{100}/\sqrt{3}$) and the effective mean pore diameter obtained by the BJH pore size analysis (desorption branch, Table 1). These values compare to wall thicknesses reported previously for similar MCM-41 materials.[17] Interestingly, no significant pore shrinkage of the thicker-walled MCM-41 **2** was observed upon calcination. As reported previously the inflection point of the type IV isotherm is shifted toward higher relative pressures in the case of the mesitylene-expanded material **2**, and capillary condensation is characterized by a pronounced hysteresis loop (Figure 2).[15] No significant hysteresis loop is found in material **1**.

*Sample **1***: C_{16}TMABr (17.3 g, 0.047 mol) was dissolved in distilled water (85.0 g, 4.72 mol) at 40 °C. Then water glass (18.0 g, 0.081 mol SiO_2, 0.047 mol NaOH) was added, and the resulting gel stirred for 20 min. Subsequent addition of portions of glycine (3.0 g, 0.040 mol) caused a drop of the pH value from 13 to 11.5. The molar composition of the resulting gel was 1 SiO_2·0.29 Na_2O·0.58 C_{16}TMABr·0.49 glycine·66 H_2O. The gel was loaded into a stoppered 125 mL PP bottle and heated without stirring at 105 °C for 45 h. No pH adjustment is necessary during hydrothermal treatment. The mixture was quenched to ambient temperature. The solid product was recovered by filtration and washed extensively with acidic ethanol and hot distilled water. After drying at room temperature the as-synthesized material was calcined and dehydrated to yield 5.8 g of material **1**.

*Sample **2***: Water glass (72.0 g, 0.324 mol SiO_2, 0.188 mol NaOH) was added to a solution of C_{16}TMABr (69.2 g, 0.188 mol) in distilled water (340.0 g, 18.9 mol), and the resulting gel stirred for 20 min. Then mesitylene (21.2 g, 0.176 mol), sulfuric acid (4.8 g, Merck, 96%) in 20 mL of distilled water, and NaCl (20.0 g, 0.342 mol) were subsequently added with stirring. The gel (pH 11; molar composition: 1 SiO_2·0.29

TABLE 1: Analytical Data, Surface Area, Pore Volume, and Pore Diameter

		elemental analysis				
sample[a]	silylating reagent(s)	wt % C	SiR_3/nm^2	a_s(BET)[b]/m^{2}g^{-1} (*C*)	V_p[c]/cm^{3}g^{-1}	d_p[d]/nm
1				1139 (80)	0.89	2.8
3a	$HN(SiMe_3)_2$	8.49	1.51	851 (26)	0.58	2.3
3a′[e]	$HN(SiMe_3)_2$	5.96	1.04	892 (43)	0.66	2.35
3b	$HN(SiHMe_2)_2$	6.95	1.85	847 (28)	0.62	2.2
3c	$HN(SiMe_2Ph)_2$	17.70	1.29	765 (23)	0.48	2.1
3d	$HN(SiMePh_2)_2$	17.26	0.74[f]	836 (36)	0.57	2.25
3e	$HN(SiMePh_2)_2$//$HN(SiHMe_2)_2$[g]	18.07	1.50	720 (20)	0.30	1.8
3f	$HN(SiMe_2CH_2\text{-})_2$	11.27	2.13	789 (21)	0.36	1.8
5a	$HN(SiMe_2n\text{-Bu})_2$	15.37	1.50	797 (13)	0.31	1.75
5b	$HN(SiMe_2n\text{-Oct})_2$	22.03	1.41	600 (40)	0.06	< 1.5
5c	$HN(SiMe_2n\text{-Oct})_2$//$HN(SiHMe_2)_2$[g]	22.12		574 (50)	0.05	< 1.5
6a	$HN(SiMe_2Vin)_2$	11.97	1.68	764 (30)	0.54	2.1
6b	$HN(SiMe_2Ph)_2$/$HN(SiMe_2Vin)_2$[h]	14.90		792 (20)	0.38	1.9
6c	$HN(SiHMe_2)_2$/$HN(SiMe_2Vin)_2$[h]	7.21		812 (28)	0.60	2.2
7a[i]	$HN(SiMe_2Vin)_2$//$BH_3(THF)$[g]	11.22		733 (37)	0.51	2.15
7b[i]	$HN(SiMe_2Vin)_2$//9-BBN[g]	26.76		582 (25)	0.20	< 1.5
2				919 (103)	0.96	3.8
4a	$HN(SiMe_3)_2$	6.02	1.24	738 (31)	0.60	3.3
4a′[e]	$HN(SiMe_3)_2$	3.36	0.66	775 (49)	0.75	3.5
8	$HN(SiMe_3)_2$//$HN(SiMe_2Vin)_2$[g]	7.03		706 (30)	0.52	2.9
9[i]	**8**//$BH_3(THF)$	10.48		611 (30)	0.41	2.6

[a] Pretreatment conditions: 250 °C, 3 h, 10^{-3} Torr. [b] Specific BET surface area (*C* = BET constant). [c] BJH desorption cumulative pore volume of pores between 1.5 and 6.5 nm diameter. [d] Pore diameter according to the maximum of the BJH pore size distribution calculated from the desorption branch. [e] Prime (′) denotes partial silylation. [f] A value of 0.70 was obtained from ^{1}H MAS NMR spectroscopy. [g] Double slant (//) denotes *consecutive* silylation. [h] Slant (/) denotes *competitive* silylation. [i] Pretreatment conditions: 25 °C, 3 h, 10^{-3} Torr.

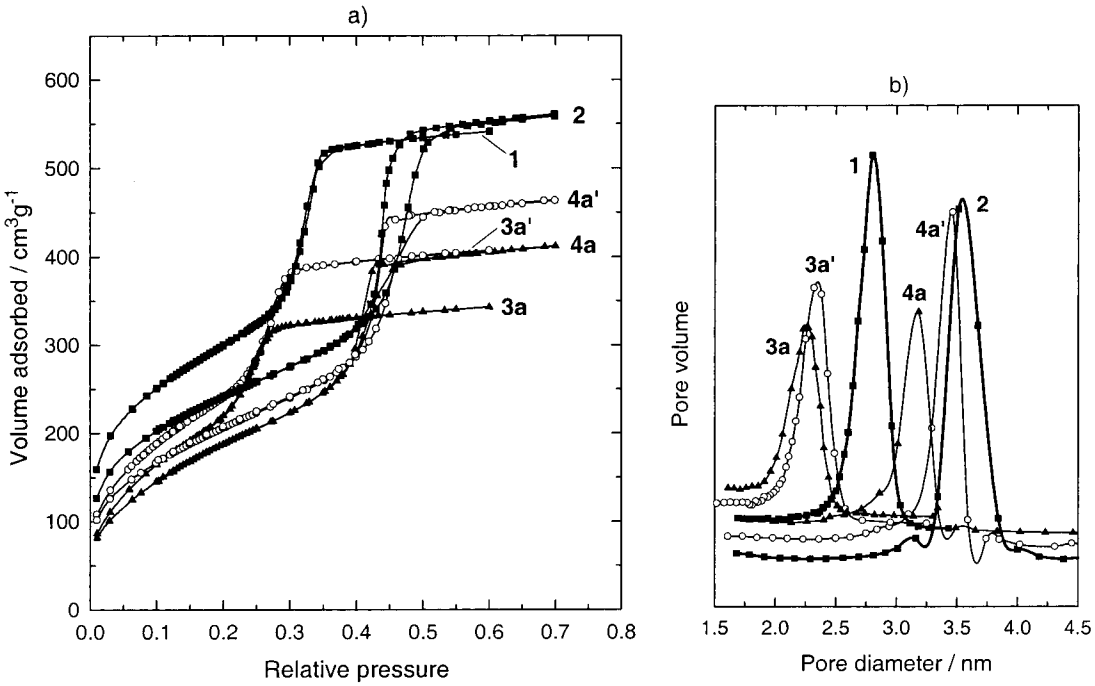

Figure 2. (a) Nitrogen adsorption/desorption isotherms on the parent (**1**, **2**: ■) and $HN(SiMe_3)_2$-silylated materials (**3a**, **3a′**: ○; **4a**, **4a′**: ▲) at 77.4 K after outgassing at 250 °C/10^{-3} Torr for 3 h. (b) Corresponding BJH pore size distributions (cf. Table 1).

Na_2O·0.58 C_{16}TMABr·0.54 mesitylene·0.15 H_2SO_4·1 NaCl·70 H_2O) was loaded into a stoppered 500 mL PP bottle, heated without stirring at 100 °C for 22 h, and processed as described above to yield 14.8 g of material **2**.

Silylation Experiments. The silylation reactions were carried out by adding the disilazane reagent diluted in 5 mL of *n*-hexane to 0.50 g of dehydrated MCM-41 material suspended in ca. 20 mL of *n*-hexane. After stirring the reaction mixture for 24 h at ambient temperature, nonreacted disilazane was separated by several *n*-hexane washings via centrifugation. The silylated materials were dried under vacuum for at least 5 h at 20 °C, then heated at 250 °C under high vacuum for 3 h if not otherwise noted in Table 1. For the *consecutive* silylation experiments, the presilylated samples were suspended in ca. 20 mL of *n*-hexane and treated with excess of the second disilazane for 24 h at ambient temperature. The *competitive* silylation experiments were performed by reacting samples of MCM-41 **1** (0.200 g) suspended in ca. 15 mL of *n*-hexane with an *n*-hexane solution of equimolar mixtures of excess silylamines for 24 h at ambient temperature. The post-synthetic treatment of the heterobisilylated materials was performed in an analogous manner to the monosilylated materials. Elemental analysis

showed that except for material **3f** no nitrogen was present in the silylated materials after thermal activation, indicating complete desorption of the ammonia produced. For carbon contents obtained from elemental analysis, see Table 1.

Hydroboration Experiments. The hydroboration reactions were carried out by contacting a suspension of a vinyl-functionalized MCM-41 sample (0.50 g) in 10 mL of THF precooled to −35 °C with 1.5 mmol (slight excess based on the reactive vinylic sites) of borane reagent. After stirring the reaction mixture for 20 h at ambient temperature, nonreacted borane reagent was removed by several washings with THF (20 mL). The resulting hybrid materials were dried *in vacuo* for at least 5 h at ambient temperature.

Characterization. *Elemental Analysis*. CHN amounts of the activated silylated samples were determined on an Elementar VarioEL (Perkin-Elmer). The surface coverage $\alpha(SiR_3)$ was calculated by the following formula ($\delta(SiR_3) = \%C(100n_CM_C)^{-1}$ [mmol g^{-1}] = concentration of surface silyl groups; %C = corrected wt % carbon referred to the parent MCM-41 silica; N_A = Avogadro constant; a_s = specific BET surface area of the dehydrated, nonmodified MCM-41 sample; n_C = number of carbon atoms per silyl group; M_C = atomic weight of carbon)

$$\alpha(SiR_3) = \delta(SiR_3)N_A a_s^{-1} \times 10^{-21}$$

[number of silyl groups per nm^2]

Due to a high degree of uncertainty of the value of the specific BET surface area, comparison of the extent of surface coverage of the differently silylated materials was drawn for samples related to the same parent material only.

Powder X-ray Diffraction (*XRD*). The X-ray diffraction measurements were performed on a Siemens D5000 instrument in the step/scan mode (step width: 0.01, accumulation time: 4.5 s/step, range (2Θ): 1.0−9.0°) using monochromatic Cu−Kα radiation.

FTIR Spectroscopy. All of the IR spectra were recorded on a Perkin-Elmer FTIR spectrometer 1760X, using Nujol mulls between CsI plates.

MAS NMR Spectroscopy. ^{1}H MAS NMR experiments were carried out at 400.13 MHz on a Bruker MSL-400 spectrometer equipped with a standard 4 mm MAS probe. Single pulse excitation has been applied (pulse repetition 5s, $\pi/2$ pulse, spinning speed 10 kHz). The ^{13}C MAS NMR spectra were recorded at 100.63 MHz in a standard 4 mm MAS probe by application of single pulse excitation with high power proton decoupling (pulse repetition 10s, $\pi/2$ pulse, spinning speed 10 kHz). All of the spectra were referenced to $Si(CH_3)_4$.

Nitrogen Adsorption. Nitrogen adsorption−desorption isotherms were measured with an ASAP 2010 volumetric adsorption apparatus (Micromeritics) at 77.4 K for relative pressures from 10^{-2} to 0.60 and 10^{-2} to 0.70, respectively [$a_m(N_2, 77\ K) = 0.162\ nm^2$]. The samples were outgassed in the degas port of the adsorption analyzer as indicated in Table 1. The BET specific surface area was obtained from the nitrogen adsorption data in the relative pressure range from 0.04 to 0.2.[18] The pore size distributions were derived from the desorption branches using the BJH method.[19]

Results and Discussion

Hexamethyldisilazane Silylation. Hexamethyldisilazane, $HN(SiMe_3)_2$ (HMDS), is the only silylamine which has been thoroughly studied as a trimethylsilylating reagent for silica materials in order to quantify the silanol number (*silanol titrator*),[20] and to compatibilize oxidic support materials for catalytic (*effect of silanol group passivation*)[21] and adsorptive (*effect of surface depolarization*) applications.[22] Hair et al. have studied the reaction of gaseous HMDS with the OH groups of silica in detail by IR spectroscopy and found a second-order kinetics with an activation energy of 18.5 kcal/mol.[10a] The liquid phase silylation reactions described herein were carried out according to Scheme 1, (3).[23] The silylated materials **3a** and **4a** were obtained by treatment of the parent materials **1** and **2**, respectively, with excess of HMDS (in the following, silylated materials are also denoted as $[MCM\text{-}41]SiR^1R^2_2$, i.e., $[MCM\text{-}41]SiMe_3$, when HMDS was the silylating reagent). Partly silylated material **3a′** was prepared by contacting material **1** with excess of silylating reagent for 5 min, followed by fast separation of nonreacted silylamine. In contrast, the degree of silylation of material **4a′** was controlled by contacting **2** with a substoichiometric amount of HMDS which corresponded to half of the surface silanol coverage.

The FTIR spectra of the partly silylated materials still show a sharp band at 3695 cm^{-1} indicative of isolated silanol groups, however, with markedly decreased intensity (not shown). After prolonged treatment with excess of HMDS, i.e., formation of materials **3a** and **4a**, the isolated silanol groups were almost completely consumed, while a considerable amount of hydrogen-bonded OH moieties (ν(OH) ca. 3660 cm^{-1}; see below, Figure 5) was left. Interestingly, the nonreacted surface silanol groups could not be detected by MAS NMR spectroscopy (see below, Figure 3). The maximum $SiMe_3$ surface coverage achieved under the prevailing reaction conditions was derived from carbon elemental analysis of **3a** as 1.51 $SiMe_3/nm^2$ (Table 1). The calculated values are in good agreement with the literature data, which were reported as 1.5 $SiMe_3/nm^2$ for the initial "fast reaction" of HMDS with predried silica in toluene at ambient temperature.[24] Apparently, the curvature of the extended pore structure in materials **1** and **2** does not have a significant effect on the $SiMe_3$ surface coverage. Nitrogen physisorption measurements on the silylated materials **3a**, **3a′**, **4a**, **4a′** clearly indicate a considerable shift of the step due to mesopore filling to smaller relative pressures (Figure 2a). The pronounced hysteresis found in material **2** is still present after silylation, although silylation significantly reduces the effective mean pore diameter, surface area, and pore volume (Table 1). The integral BJH pore size distributions derived herefrom reveal effective pore size engineering (Figure 2b). Narrower pore size distributions are observed for the silylated samples of the mesitylene-expanded material, probably due to a surface smoothing effect.[25]

The most peculiar feature of these silylation experiments is the regularly proceeding modification of the entire material, rendering uniformly modified mesopores. This effect can be assigned to the low-rate surface reaction of HMDS. We have noticed earlier[26] that under the same conditions substoichiometric treatment of a sample of MCM-41 with more reactive organometallic reagents such as trimethylaluminum proceeds in a different manner, producing both modified and nonmodified mesopores.

Variation of the Lateral Extension of the Disilazane Reagent. To probe the impact of differently sized/shaped groups on surface coverage, mixed alkyl/hydride and alkyl/phenyl substituted disilazanes, respectively, were contacted with dehydrated MCM-41 **1** for 24 h in *n*-hexane suspensions (Scheme 1, (3)). The resulting silylated materials **3b**−**d** display surface coverages ranging from 0.74 to 1.85 SiR_3/nm^2 as derived from carbon elemental analysis (Table 1). Tetramethyldisilazane, $HN(SiHMe_2)_2$ (TMDS), carrying the least bulky silyl group produces the highest surface coverage in material **3b**, which

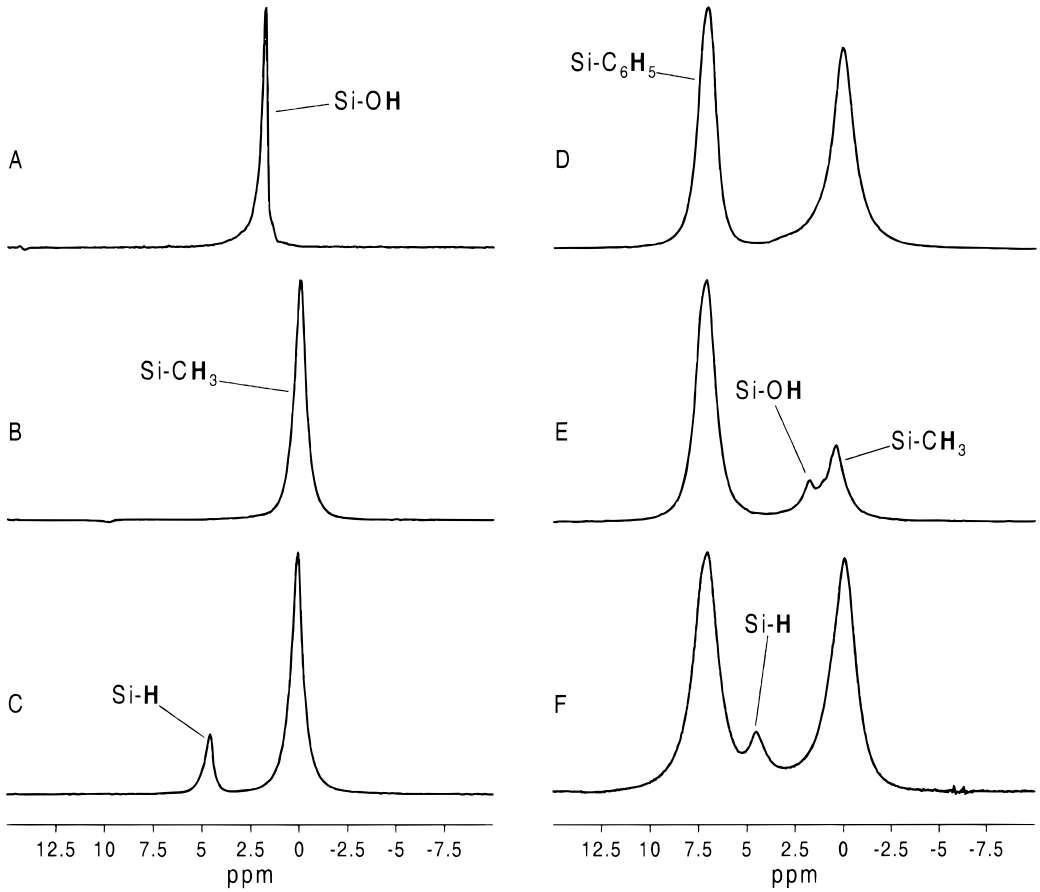

Figure 3. ^{1}H MAS NMR spectra of nonmodified and silylated samples: (A) MCM-41 dehydrated at 280 °C/10^{-5} Torr (**1**); (B) [MCM-41]$SiMe_3$ (**3a**); (C) [MCM-41]$SiHMe_2$ (**3b**); (D) [MCM-41]$SiMe_2Ph$ (**3c**); (E) [MCM-41]$SiMePh_2$ (**3d**); (F) [MCM-41]$(SiMePh_2)(SiHMe_2)$ (**3e**). All of the silylated samples were measured after pretreatment at 250 °C/10^{-3} Torr.

value is ca. 20% higher than that achieved with the standard silylating reagent HMDS. This higher silylation efficiency should qualify TMDS as a more efficient reagent for silanol deactiviation/passivation processes. The $SiMePh_2$-silylated material **3d**, [MCM-41]$SiMePh_2$, displays the lowest surface coverage of 0.74 SiR_3/nm^2, reflecting the presence of two bulky phenyl substituents per silyl group. All of the silylated materials have been characterized by solid state ^{1}H and ^{13}C NMR spectroscopy using magic-angle-spinning techniques (MAS). The ^{1}H MAS NMR spectra of the materials **3a**−**c** (Figure 3, B−D) show the disappearance of the proton resonance of the isolated SiOH groups of dehydrated MCM-41 material **1** which is located at 1.8 ppm (Figure 3, A). The chemical shifts of the silyl groups can be assigned to Si−CH_3 (0.1 ppm), Si−H (4.6 ppm), and Si−C_6H_5 groups (7.1 ppm). The spectrum of material **3b** (Figure 3, C) also revealed the Si−H moiety to constitute an excellent spectroscopic probe which proved to be stable under the prevailing reaction conditions and subsequent thermal treatment. The ^{1}H MAS NMR spectrum of material **3d** is more complex (Figure 3, E). At least three resonances located at 0.5, 1.8, and 7.2 ppm with relative signal intensities of 2.7:1.0:9.4 were observed. The signal at 1.8 ppm reflects a considerable amount of residual silanol groups. The steric bulk/shape of silyl groups carrying two phenyl rings seems to markedly affect the surface reaction and hence the extent of silanol group consumption.

The ^{13}C MAS NMR spectra of **3a** (Figure 4, A) and **3b** (not shown) contain a single signal of the SiMe carbon atoms at 0 ppm, while those spectra of materials **3c** and **3d** confirm the findings of a monofunctional surface reaction (Figure 4, B and C). Four signals in a ratio of 1(ipso):2 (ortho):2 (meta):1 (para) of the phenyl substituents appeared well resolved in the range of 120−140 ppm. As expected, the intensity of the SiMe signal at 0 ppm is significantly decreased in material **3d** compared to **3c**.

These findings could be further clarified by FTIR spectroscopy. The SiO−H region of the dehydrated material **1** is dominated by a sharp and intensive vibration of isolated silanol groups at 3695 cm^{-1} (Figure 5, A).[27,28] This band is completely consumed in material **3b** by the sterically least demanding tetramethyldisilazane (not shown), which behavior is in accord with the aforementioned highest surface coverage of the $SiHMe_2$ group. Additionally, the IR spectrum of material **3b** contains a strong band at 2145 cm^{-1} assignable to the SiH stretch vibration. A small amount of isolated and hydrogen-bonded SiOH moieties [ν(OH) ca. 3660 cm^{-1}] seems to be inaccessible to the silylating reagents $HN(SiMe_3)_2$ (**3a**) and $HN(SiMe_2Ph)_2$ (**3c**) (Figure 5, B and C), which is also revealed by the decreased surface coverage of 82% and 70%, respectively. Interestingly, the band maximum of material **3c** is shifted to 3616 cm^{-1}. This behavior is even more pronounced in material **3d** (Figure 5, D) which shows a surface coverage as low as 40%. In addition to a pronounced ν(OH) band at 3695 cm^{-1}, a relatively more intense and sharp OH stretch vibration is detected at 3616 cm^{-1}. The latter band is due to the interaction of residual silanol groups with silicon-attached phenyl groups. For comparison, a similar shift of the ν(OH) band is observed when dry toluene is adsorbed onto dehydrated material **1** (not shown). Similar effects have not been discussed for a MCM-41 sample which was partly dehydrated at 100 °C and treated with triphenylchlorosilane in

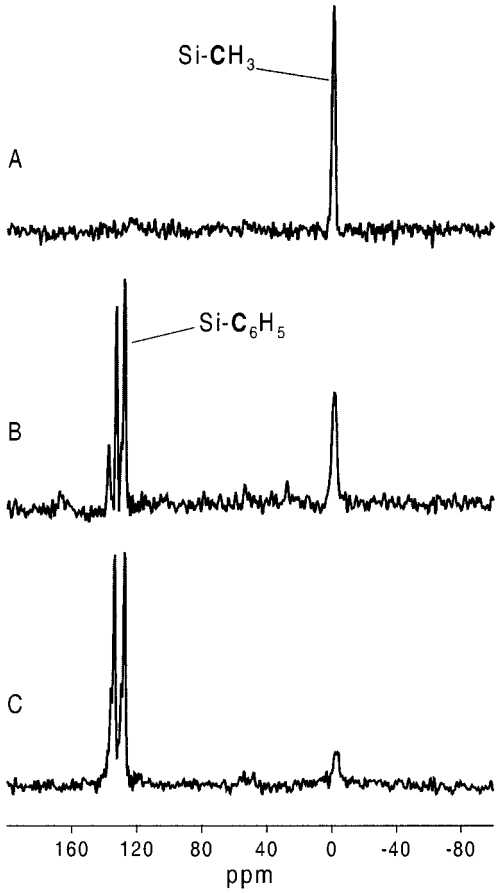

Figure 4. ^{13}C MAS NMR spectra of the silylated samples [MCM-41]$SiMe_3$ (**3a**, A), [MCM-41]$SiMe_2Ph$ (**3c**, B), and [MCM-41]$SiMePh_2$ (**3d**, C) after outgassing at 250 °C/10^{-3} Torr for 3 h.

hot toluene for 48 h.[8a] The aromatic ν(CH) and ν(C═C) at 3072 and 3050 and 1592 cm^{-1}, respectively, are clearly visible in materials **3c** and **3d**.

The silylated materials **3a**−**d** display adsorption/desorption isotherms of type IV according to the IUPAC nomenclature.[18] The isotherms are characterized by a sharp inflection point at relative pressures p/p_o, ranging from 0.18 to 0.25, as shown for materials **3b**−**3d** in Figure 6. The BJH differential pore size distribution and the effective mean pore diameter (2.1−2.3 nm), respectively, reveal the change of the pore size. Also, the BET surface areas were considerably decreased upon silylation. The isotherm of material [MCM-41]$SiMePh_2$ (**3d**) corresponds to a comparatively high pore volume, which refers to the distinct reaction behavior of the corresponding disilazane reagent (low surface coverage).

The elemental analyses and ^1H MAS NMR and IR spectroscopic findings of material **3d** give important details of the surface silanol distribution. It can be concluded that approximately 80% of the ca. 60% of nonsilylated Si−OH groups are located below an aromatic π-system as schematically redrawn in Scheme 2. Consequently, the distance of the OH groups lies predominantly between 2 and 4.7 Å, a range which corresponds to a position below a phenyl ring as derived from simple molecular modeling studies.[29] Considering a maximum surface coverage of ca. 1.85 OH/nm^2 (as obtained from TMDS silylation, Table 1) a mean (OH)···(OH) distance of ca. 7.4 Å would result. Hence, our qualitative findings suggest a rather irregular distribution of the surface silanol groups and probably the presence of silanol nests. A subsequent silylation experiment shows that most of these nonreacted silanol groups present in material **3d** are accessible to the sterically least demanding reagent $HN(SiHMe_2)_2$ (Scheme 2). The surface coverage of the resulting heterobisilylated material **3e** is approximately 1.41 SiR_3/nm^2 as derived from ^1H MAS NMR spectroscopy ($SiHMe_2$:$SiMePh_2$ = 1:1.1; Figure 3, F). This is in accordance with the IR spectrum of material **3e** indicating the complete consumption of the isolated silanol groups at 3695 cm^{-1} and the survival of a weak band at 3616 cm^{-1} (Figure 5, E). Again,

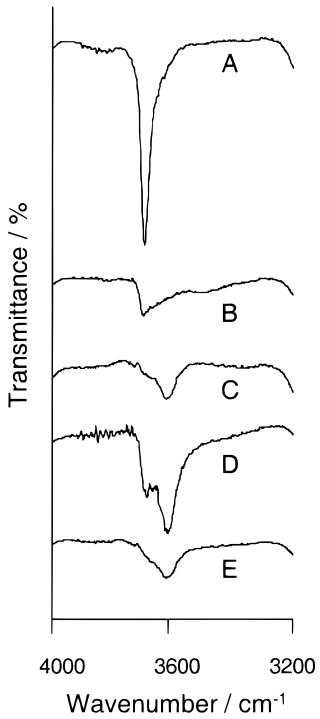

Figure 5. Region of the OH stretch vibration of the parent (**1**, A) and the silylated materials [MCM-41]$SiMe_3$ (**3a**, B), [MCM-41]$SiMe_2Ph$ (**3c**, C), [MCM-41]$SiMePh_2$ (**3d**, D), and [MCM-41]$SiMePh_2$//$SiHMe_2$ (**3e**, E) after outgassing at 250 °C/10^{-3} Torr for 3 h. The IR spectra were recorded as a Nujol mull.

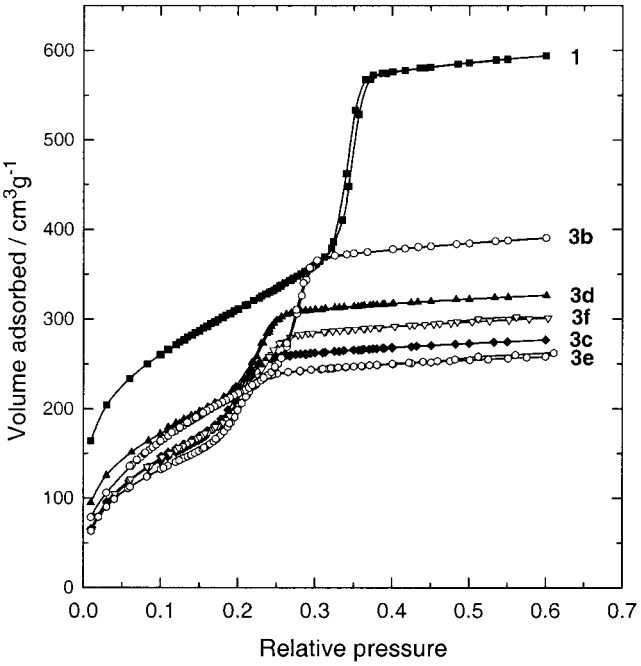

Figure 6. Nitrogen adsorption/desorption isotherms on the parent (**1**: ■) and silylated materials **3b** (○), **3c** (◆), **3d** (▲), **3e** (⬡), and **3f** (▽) at 77.4 K after outgassing at 250 °C/10^{-3} Torr for 3 h (cf. Table 1).

SCHEME 2. Formation of Heterobisilylated Material 3e via *Consecutive* Silylation (effect of aryl···OH interaction)

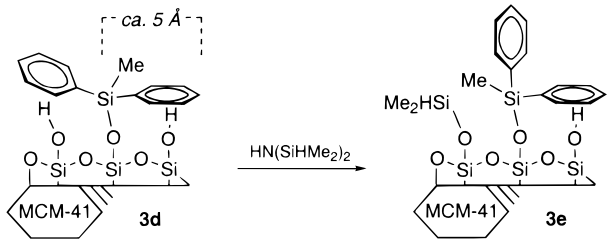

the latter feature was not detectable by MAS NMR spectroscopy in the form of a silanol proton signal. This *consecutive* silylation further decreases the surface area, pore volume, and mean pore diameter as revealed by its nitrogen adsorption/desorption behavior. These findings suggest a reorientation of the immobilized silyl groups in such way that the bulky phenyl groups in **3e** tentatively point away from the pore walls.

The spacing of the surface silanol groups could be further examined by the application of another specialized silylamine, cyclic $HN(SiMe_2CH_2CH_2SiMe_2)$, to yield material **3f** (Scheme 3). Neighbored silanol groups as detected in material [MCM-41]$SiMePh_2$ (**3d**) should produce ring siloxane surface species of type **A** since the initially formed covalently surface bound primary silylamine (species **B**) should react much faster than its cyclic precursor. CH analysis and a calculated surface coverage of 2.13 $\{[MCM\text{-}41](SiMe_2CH_2CH_2SiMe_2)[MCM\text{-}41]\}_{0.5}/nm^2$ favor **A** as the predominant surface species, though the presence of another silylation product, probably species C, cannot be ruled out on the basis of the nitrogen analysis (0.4 wt % N) and of the IR spectrum of **3f** which indicated a weak NH stretch vibration at 3388 cm^{-1} (not shown). In addition, the ^1H MAS NMR spectrum of **3f** shows a nonresolved signal for the methyl and methylene protons (Figure 7, A), indicating a limited mobility of the silyl groups which would also suggest **A** as the predominant species. The ^{13}C MAS NMR spectrum of **3f** reveals separated signals for the methyl and methylene carbon atoms at −2.3 and 9.3 ppm, respectively (Figure 7, B). From the nitrogen physisorption data of material **3f** it is also clear that the pore volume and diameter in the mesopore regime are considerably reduced in comparison to material **3a** (Table 1, Figure 6), pointing out the presence of bulkier silyl groups such as represented by species of type **B** and **C**.

SCHEME 3. Possible Surface Species upon Silylation of Dehydrated MCM-41 with the Cyclic Silylamine $HN(SiMe_2CH_2-)_2$

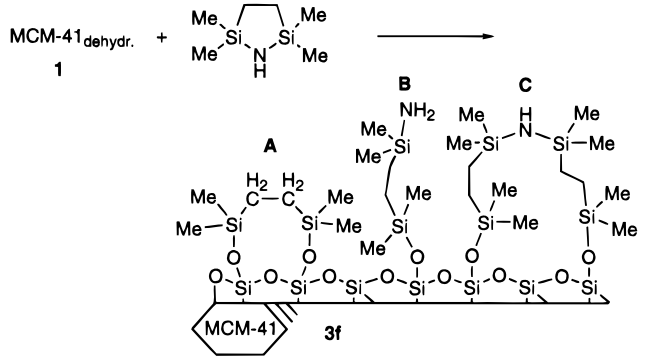

In a previous contribution we also reported on the behavior of the silylated materials **3a**, **3c**, and **3d** in both the competitive H_2O/toluene adsorption (Hydrophobicity Indices) and the single-component adsorption of *tert*-butyl alcohol.[11] Both of these studies revealed that the sorption capacity, i.e., the amount and accessibility of surface silanol groups, decreases in the order MCM-$41_{dehydr.}$ (**1**) ≫ [MCM-41]$SiMePh_2$ (**3d**) > [MCM-41]-$SiMe_2Ph$ (**3c**) ≈ [MCM-41]$SiMe_3$ (**3a**).

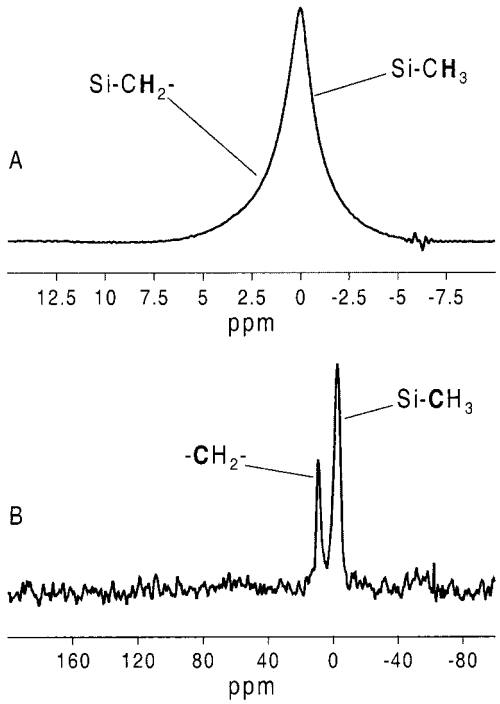

Figure 7. ^1H (A) and ^{13}C MAS NMR spectra (B) of the silylated sample [MCM-41]$(SiMe_2CH_2CH_2SiMe_2)$[MCM-41] (**3f**) after outgassing at 250 °C/10^{-3} Torr for 3 h.

Variation of the Longitudinal Extension of the Disilazane Reagent. The effect of the alkyl chain length of a dimethyl-*alkyl*silyl group on the surface coverage and pore texture was examined using 1,3-di-*n*-butyltetramethyldisilazane and 1,3-di-*n*-octyltetramethyldisilazane. The resulting silylated samples [MCM-41]$SiMe_2$(*n*-Bu) (**5a**) and [MCM-41]$SiMe_2$(*n*-Oct) (**5b**) reveal a surface coverage similar to that of material [MCM-41]$SiMe_3$ (**3a**) (Table 1). Recently, Jaroniec et al.[30] reported markedly lower values of 1.24 and 1.08 silyl groups/nm^2 for corresponding materials obtained by the reaction of *n*-butyldimethylchlorosilane and *n*-octyldimethylchlorosilane, respectively, with a sample of MCM-41 in refluxing anhydrous pyridine. For comparison, their MCM-41 material was dehydrated even at a lower temperature of 423 K (no vacuum applied) prior to the reaction with the chlorosilanes. In addition, the more drastic reaction conditions are prone to multifunctional surface reactions. We found that a considerable amount of isolated silanol groups is still present in materials **5a** and **5b** as indicated by a sharp IR band at 3695 cm^{-1} (not shown). The ^1H MAS NMR spectra of **5a** (A) and **5b** (B) shown in Figure 8 consist of three overlapping lines. The experimental spectra (upper trace) could be simulated (middle trace) by Lorentzian lines (lower trace). On the basis of this simulation the chemical shifts of the silylmethyl, methyl, and methylene groups could be assigned as 0, 0.8, and 1.2 ppm, respectively. In both samples the relative line intensities of $SiCH_3$:CH_3:CH_2 (**5a**, 1:2:2; **5b**, 1:5:2) are in good agreement with the theoretical values. The ^{13}C MAS NMR spectra of **5a** and **5b** show well-separated signals allowing an unambiguous peak assignment (Figure 9, A and B; Table 2). These values are in good analogy with literature reports on dimethylalkyl silylated silica gels.[31]

According to the nitrogen physisorption measurement, the pore volume and mean pore diameter of materials **5a** and **5b**

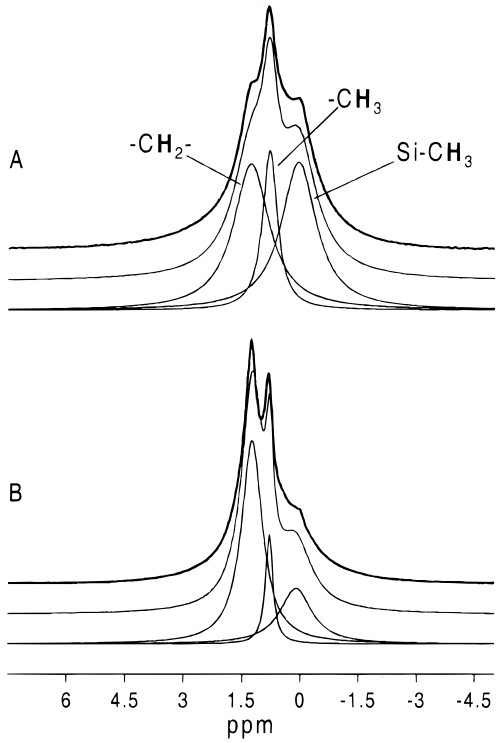

Figure 8. ^{1}H MAS NMR spectra of the silylated samples [MCM-41]-$SiMe_2$(*n*-Bu) (**5a**, A) and [MCM-41]($SiMe_2$(*n*-Oct) (**5b**, B) after outgassing at 250 °C/10^{-3} Torr for 3 h.

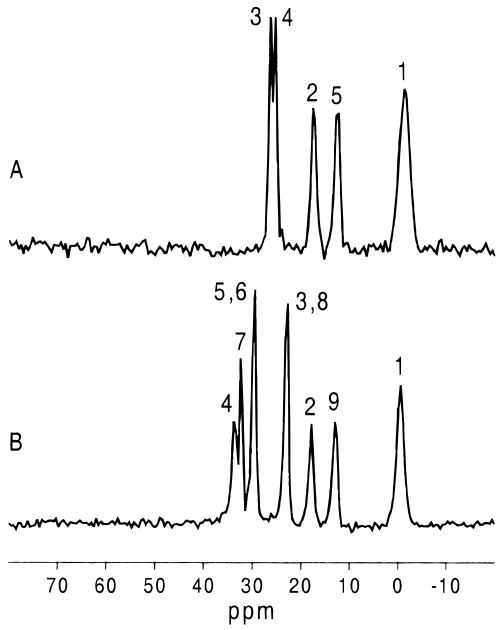

Figure 9. ^{13}C MAS NMR spectra of the silylated samples [MCM-41]$SiMe_2$(*n*-Bu) (**5a**, A) and [MCM-41]($SiMe_2$(*n*-Oct) (**5b**, B) after outgassing at 250 °C/10^{-3} Torr for 3 h (cf. Table 2).

decreased significantly depending on the length of the alkyl chain. Apparently, the longer hydrophobic aliphatic chains are orientated toward the center of the pore, thus reimaging the final step of the formation of mesoporous host material via a cooperative surfactant/silicate self-assembly mechanism.[32] While material **5a** shows the characteristic type-IV isotherm, the *n*-octyl-functionalized material **5b** approaches a type-I isotherm (Figure 10). In addition, the isotherm of material **5b** seems to be irreversible at relative pressures below 0.2. The appearance of such a low-pressure hysteresis has been reported recently by

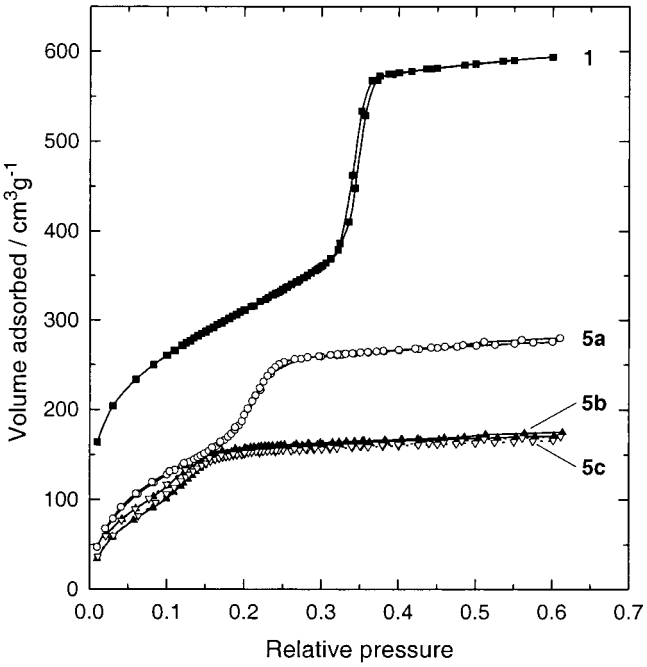

Figure 10. Nitrogen adsorption/desorption isotherms on the parent (**1**: ■) and the silylated materials **5a** (○), **5b** (▲), and **5c** (▽) at 77.4 K after outgassing at 250 °C/10^{-3} Torr for 3 h (cf. Table 1).

TABLE 2: ^{13}C MAS NMR Peak Assignment of Materials 5a, 5b and 7b

Sample	^{13}C chemical shift / ppm		Figure
5a	C1	-1.1	9/A
1 2 3 4 5	C2	17.5	
≡Si–O–Si$(CH_3)_2$–CH_2–CH_2–CH_2–CH_3	C3	26.5	
	C4	25.5	
	C5	12.4	
5b	C1	-0.4	9/B
1 2 3 4 5 6 7 8 9	C2	19.0	
≡Si–O–Si$(CH_3)_2$–CH_2–CH_2–CH_2–CH_2–CH_2–CH_2–CH_2–CH_3	C3,8	23.0	
	C4	33.5	
	C5,6	29.5	
	C7	32.4	
	C9	14.0	
7b	C1	-0.1	15/C
1 2 3 4 5 6	C2	19.8	
≡Si–O–Si$(CH_3)_2$–CH_2–CH_2–B[$(CH)_2$–$(CH_2)_4$–$(CH_2)_2$]	C3	10.1	
	C4	23.2	
	C5	33.8	
	C6	31.9	

Jaroniec et al.[30] for similarly *n*-octyl-functionalized MCM-41 materials and discussed as a possible result of a very weak interaction between adsorbed nitrogen and long aliphatic chains, or alternatively as an interaction between nitrogen with high-energy adsorption sites of the silica surface.[30] Subsequent HN-$(SiHMe_2)_2$ silylation of material **5b** removes almost all of the residual silanol groups to form heterobisilylated material **5c**. An FTIR peak at 2145 cm^{-1} confirmed the presence of covalently linked $SiHMe_2$ moieties. However, the characteristic low-pressure hysteresis is still present which possibly outrules a specific effect of the residual silanol groups on the physisorption behavior of nitrogen and hence on the peculiar appearance of the isotherm.

Use of Vinyl-Functionalized Disilazane Reagents − Competitive Silylation Reactions. The modification of silica surfaces with silyl groups carrying valuable functional groups is a popular approach to tailor support materials for, e.g., catalytic applications.[8,9] In addition to phenyl[33] and SiH functionalities described above,[34] the vinyl moiety can be readily grafted onto the surface via silazane silylation.[11] Recently, vinyl functionalities have been incorporated into silica materials also via hy-

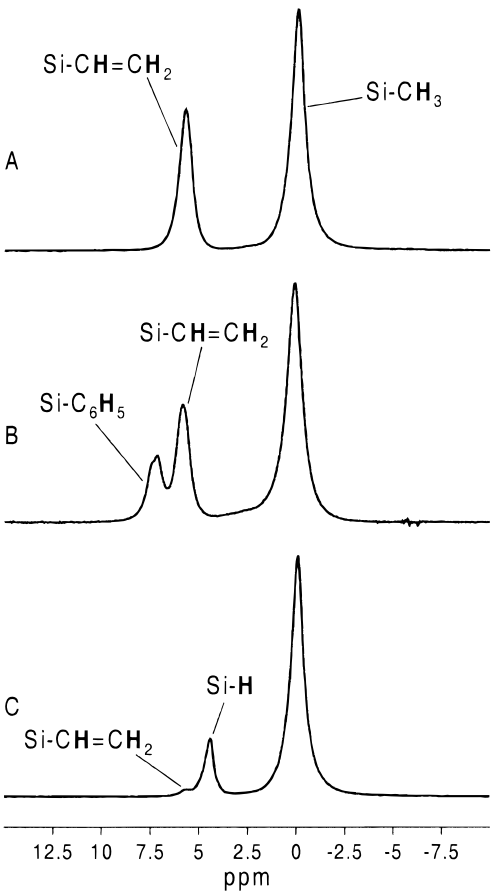

Figure 11. ^{1}H MAS NMR spectra of the silylated samples [MCM-41]$SiMe_2Vin$ (**6a**, A), [MCM-41]$SiMe_2Ph/SiMe_2Vin$ (**6b**, B), and [MCM-41]$SiHMe_2/SiMe_2Vin$ (**6c**, C) after outgassing at 250 °C/10^{-3} Torr for 3 h.

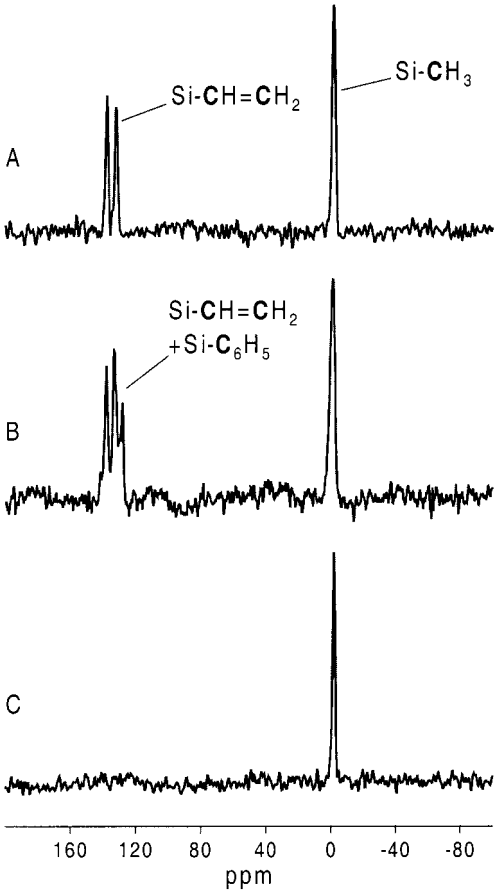

Figure 12. ^{13}C MAS NMR spectra of the silylated samples [MCM-41]$SiMe_2Vin$ (**6a**, A), [MCM-41]$SiMe_2Ph/SiMe_2Vin$ (**6b**, B), and [MCM-41]$SiHMe_2/SiMe_2Vin$ (**6c**, C) after outgassing at 250 °C/10^{-3} Torr for 3 h.

drothermal synthesis using mixtures of silica precursor compounds.[4c,35] Vinyl functionalities exhibit broad reactivity and display versatile precursor moieties for both subsequent organic transformations and metal incorporation reactions as evidenced, e.g., in hydrometalation and olefin metathesis reactions. Metal incorporation reactions have been studied particularly in the case of model compounds for oxo surfaces as represented by the class of oligosilsesquioxanes which are incompletely condensed alkylsilantriols.[36] Reaction of dehydrated **1** with excess of HN-$(SiMe_2Vin)_2$ yields material [MCM-41]$SiMe_2$(Vin) (**6a**) featuring a surface coverage of 1.68 $(SiMe_2Vin)/nm^2$ similar to that of the $SiMe_3$-silylated material **3a**. Spectroscopic investigations confirm the Si-vinyl group to be readily detectable and to be stable under the prevailing reaction conditions and subsequent thermal treatment. While a sharp $(C{=}C)_{vin}$ stretch vibration is clearly visible in the IR spectrum at 1597 cm^{-1} (not shown), the ^{1}H MAS NMR spectrum shows the methyl (0 ppm) and the vinyl protons (5.7 ppm) in the correct integral ratio of 2:1 (Figure 11, A). The ^{13}C MAS NMR spectrum shows besides the SiMe peak at 0 ppm the signals of the vinyl group at 131.6 ppm ($=CH_2$) and 137.4 ppm ($-CH=$) (Figure 12, A).

Competitive silazane silylation, i.e., treatment of dehydrated MCM-41 **1** with excess of equimolar mixtures of silylamines, was found as an effective means to direct the relative number of the surface vinyl functionalities (Scheme 4). ^{1}H MAS NMR spectroscopy allowed a quantitative analysis of the signal intensities present in these heterobisilylated materials. The HN-$(SiMe_2Ph)_2/HN(SiMe_2Vin)_2$ reaction yielded material **6b** revealing relative line intensities of 1:1.9 of the phenyl group at 7.2 ppm and the vinyl group at 5.8 ppm (Figure 11, B). This accounts for a surface silylation with ca. 75% of vinyl-functionalized and 25% of phenyl-functionalized sites. In contrast, the $HN(SiHMe_2)_2/HN(SiMe_2Vin)_2$ reaction gave mate-

SCHEME 4. ***Competitive Silylation*** **− Influence of the Steric Bulk of the Silyl Group**

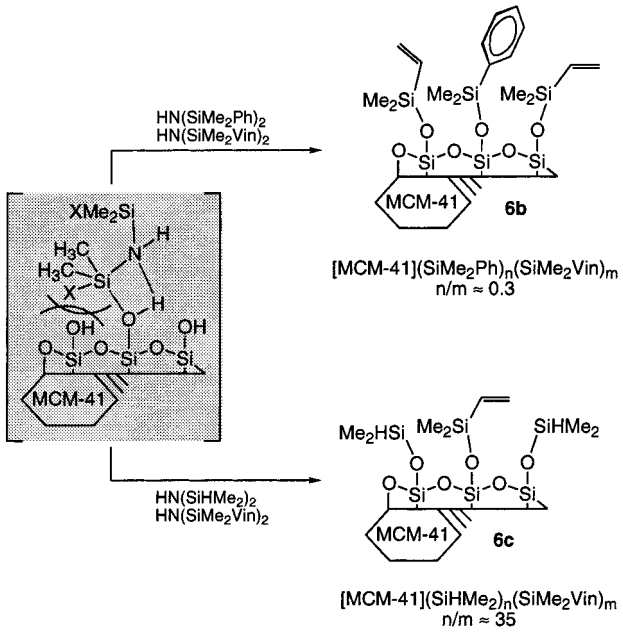

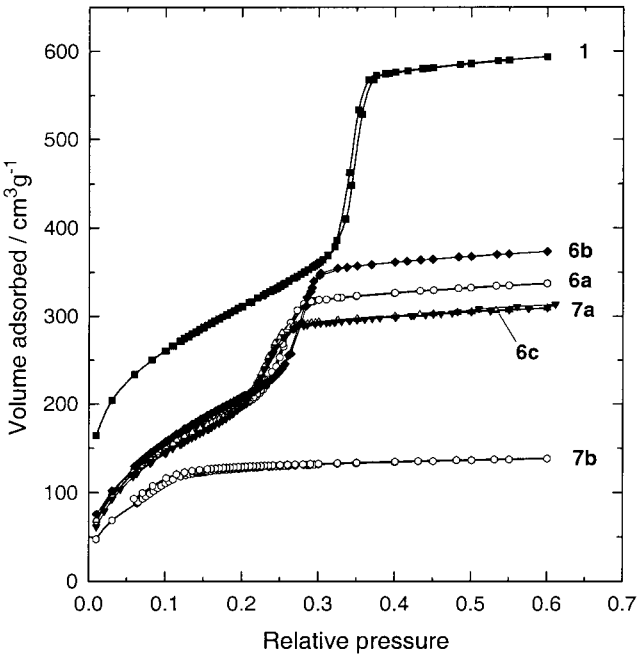

Figure 13. Nitrogen adsorption/desorption isotherms on the parent (**1**: ■), the silylated materials **6a** (○), **6b** (◆), and **6c** (△) (after outgassing at 250 °C/10^{-3} Torr for 3 h), and hydroborated materials **7a** (▼) and **7b** (⬡) (after outgassing at 25 °C/10^{-3} Torr for 3 h) at 77.4 K (cf. Table 1).

rial **6c** with a markedly decreased signal for the vinyl protons relative to the silane protons (I_{vin}:I_{SiH} = 1:14.6, Figure 11, C). Hence, in material **6c** only 2% of the silyl groups are carrying a vinyl functionality. The ^{13}C MAS NMR vinyl and phenyl signals of material **6b** overlap (Figure 12, B). Although it is clear that the vinyl groups are the predominant species, a better quantification is obtained on the basis of the ^{1}H MAS NMR spectrum. In material **6c** only the $SiMe_3$ group could be detected by ^{13}C MAS NMR spectroscopy due to the low concentration of the vinyl carbon atoms (Figure 12, C).

These competitive silylation reactions provide important mechanistic details and confirm the dependency of the reaction rate on the steric bulkiness of the silyl groups of the silylamine. The preformation of a four-centered "O···H···N···Si" transposition as depicted in Scheme 4 apparently displays the rate-determining step of this peculiar silylation reaction.[10,24] Less bulky groups such as $SiHMe_2$ favor (i) a proper orientation, (ii) deprotonation of the surface silanol groups, and (iii) silyl group transfer. Such a sterically crowded four-centered transposition is also in accord with the higher surface coverage in the presence of the smaller silyl group. Elemental analysis and nitrogen physisorption data of all vinyl-functionalized materials are summarized in Table 1. All of the materials **6** display type-IV isotherms and show the expected shift of the inflection point toward smaller relative pressures corresponding to a significant decrease of pore volume and mean pore diameter (Figure 13). The number of surface vinyl groups could also be affected by reacting presilylated material [MCM-41]$(SiMe_3)_x(OH)_y$ (**4a′**) with $HN(SiMe_2Vin)_2$ to give material **8** (see below).

Modification of Vinyl-Functionalized MCM-41 via Hydrometalation. To probe the accessibility and reactivity of the surface vinyl functionalities, hydroboration reactions were performed using BH_3(THF) and 9-BBN in THF at ambient temperature (Scheme 5). 9-BBN is commonly employed to direct the regioselectivity of this addition process, generating B−C bonds at the sterically less encumbered carbon atom (isomer **A**).[37] Siliceous materials modified with boron compounds are discussed as promising Lewis acidic catalysts.[7] The hydroborated materials **7a** and **7b** obtained from material **6a** were characterized by elemental analysis (Table 1), FTIR (spectra not shown), and ^{1}H MAS NMR spectroscopy. The characteristic C═C stretching frequency at 1597 cm^{-1} [4c,38] was completely consumed upon addition of BH_3(THF). New vibration modes appeared at 2507 and 1558 cm^{-1} which are assigned to B−H and B−H−B bridge stretching frequencies.[39] Formation of the BH_3(THF) addition product **7a** was confirmed by the ^{1}H MAS NMR spectrum due to the complete disappearance of the vinylic protons at 5.7 ppm (Figure 14, B). A broad resonance centered at 0.1 ppm appeared which originates from overlapping resonances of Si−CH_3 and B−H protons. The broadening of the signal is probably due to the coexistence of different addition

SCHEME 5. Hydroboration of Vinyl-Functionalized MCM-41

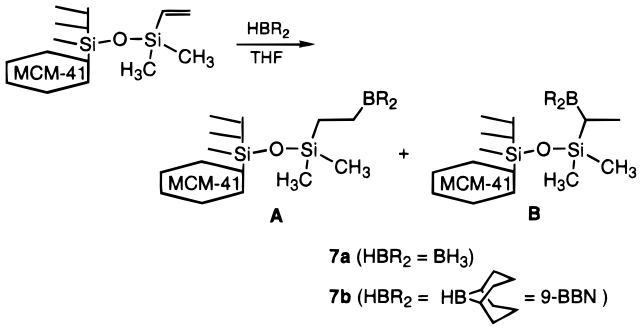

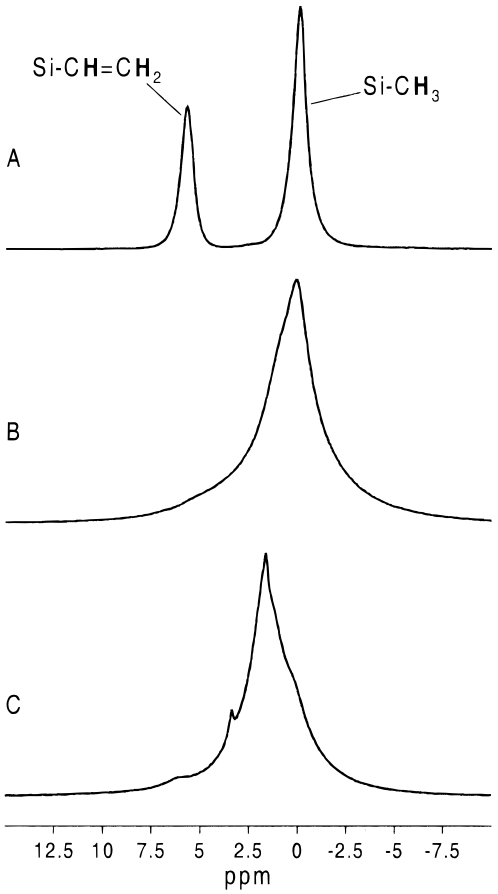

Figure 14. ^{1}H MAS NMR spectra of the vinyl-functionalized sample [MCM-41]$SiMe_2$Vin (**6a**, A, after outgassing at 250 °C/10^{-3} Torr for 3 h) and the hydroborated materials [MCM-41]$SiMe_2$Vin//BH_3(THF) (**7a**, B) and [MCM-41]$SiMe_2$Vin//9-BBN (**7b**, C) after outgassing at 25 °C/10^{-3} Torr for 3 h.

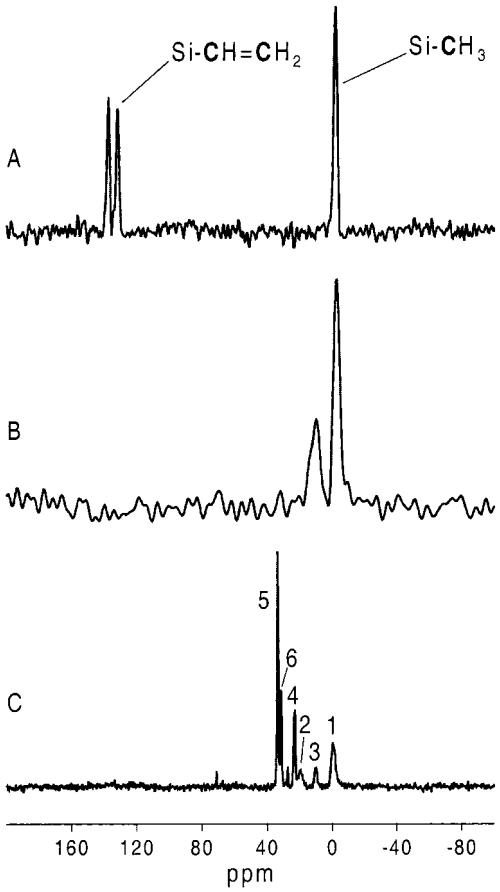

Figure 15. ^{13}C MAS NMR spectra of the vinyl-functionalized sample [MCM-41]$SiMe_2Vin$ (**6a**, A, after outgassing at 250 °C/10^{-3} Torr for 3 h) and the hydroborated materials [MCM-41]$SiMe_2Vin$//BH_3(THF) (**7a**, B) and [MCM-41]$SiMe_2Vin$//9-BBN (**7b**, C, cf. Table 2) after outgassing at 25 °C/10^{-3} Torr for 3 h.

products "R−BH_2", including the stereoisomers **A** and **B** (Scheme 5). The formation of Lewis acid/base derived surface species of type "(Si_2O)→(BH_3)" cannot be ruled out. The appearance of the resonance at 5.7 ppm in the ^1H MAS NMR spectrum of material **9** (Figure 14, C) reveals that the reaction with 9-BBN renders a significant amount of vinylic protons nonmodified. The limited reaction is probably due to steric restrictions at the surface, supporting an anti-Markovnikov addition of the borane to produce isomer **A** (Scheme 5). The peaks at 3.4 and 1.7 ppm result from the CH and CH_2 protons of the immobilized 9-BBN group which are superimposed by the broader resonances of Si−CH_2−CH_2−BR_2 and Si−CH_3 protons, the maximum of the latter being pronounced by the shoulder at about 0 ppm. The ^{13}C NMR spectra of materials **7a** and **7b** show the complete disappearance of the vinyl carbon atoms (Figure 15, B and C). For material **7a** a new signal at 10 ppm with a shoulder at 14 ppm appeared attributable to the borylated ethyl group. The signal shape could not be simulated by two separated signals, probably due to the presence of a mixture of isomers **A** and **B** (Scheme 5). The ^{13}C NMR spectrum of material **7b** shows in addition to the three resonances of the 9-BBN fragment, two signals for the silicon bonded CH_2CH_2 group, and one signal for the $SiMe_3$ group (Table 2). The presence of a small amount of THF is indicated by two resonances at 71.2 and 27.5 ppm.

The steric bulk of the 9-BBN moiety considerably decreases the pore volume of the hybrid material **7b** as evidenced by nitrogen physisorption (Table 1, Figure 13). The resulting

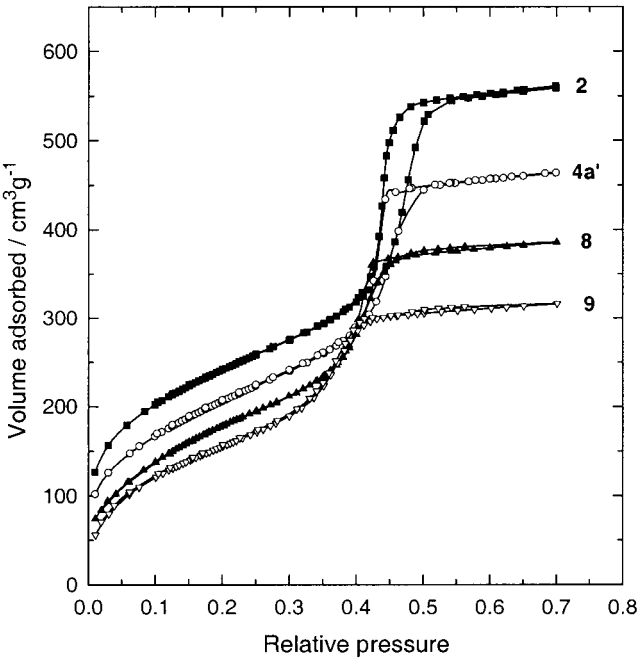

Figure 16. Nitrogen adsorption/desorption isotherms on the parent (**2**: ■), the silylated materials **4a′** (○) and **8** (▲), and the hydroborated material **9** (▽) at 77.4 K after outgassing at 250 °C/10^{-3} Torr and 25 °C/10^{-3} Torr, respectively, for 3 h (cf. Table 1).

isotherm shows in addition to the disappearance of the mesopore filling step a low-pressure hysteresis comparable to that of hybrid material **5b**. Addition of the smaller BH_3 group implies only a slight drop in pore volume and effective mean pore diameter, respectively; the original type-IV isotherm is retained.

The amount of silyl group-bonded boron species could be varied through control of the preceding 1,3-divinyltetramethyldisilazane reaction. The controlled generation of covalently linked vinyl groups could be achieved either by *competitive* silylation or by *consecutive* treatment with silylamines HN-($SiMe_3$)$_2$ and HN($SiMe_2Vin$)$_2$. The latter silylation sequence as shown in Scheme 6 was conducted with pore-expanded MCM-

SCHEME 6. The Silylation/Hydroboration Sequence Involving *Consecutive* Silylation

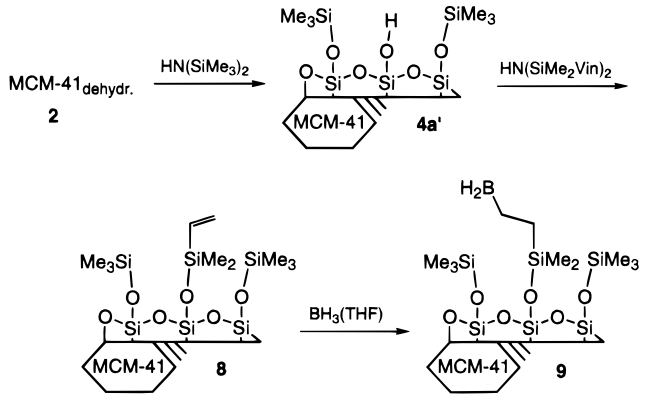

41 material **2** producing the partly monosilylated sample **4′** and the fully heterobisilylated material **8**. Subsequent hydroboration with BH_3(THF) gave material **9**. Nitrogen physisorption measurements revealed the stepwise mesopore filling occurring during such a high-yield multistep grafting process (Figure 16). While the hysteresis loop due to capillary condensation is clearly visible for the silylated samples **4a′** and **8**, further decrease of

the pore diameter by hydroboration gave an almost reversible isotherm for material **9**. Apparently, the nitrogen miniscus becomes unstable at cylindrical pore widths < ca. 2.6 nm. Ongoing investigations in our laboratory show that, according to the above scenario, boron reagents can act as molecular adaptors between a vinyl-functionalized oxo surface and a vinyl-substituted metallocene complex. Controlled metallocene immobilization on oxidic support materials is still a major topic in Ziegler−Natta-type polymerization catalysis.[40,41]

Conclusions

Disilazane reagents represent an effective "silylation pool" to study and to modify the surface morphology of mesoporous silica materials. Nitrogen physisorption measurements and MAS NMR spectroscopy proved very useful to characterize the peculiarities of these surface silylation reactions including the effect of pore size engineering, the monofunctional reaction behavior, and the organic structure of the immobilized silyl groups. The surface coverage and hence the silylation efficiency is directed by size/shape effects of the organic substituent of the silyl moiety introduced. We have shown that tetramethyldisilazane affords the highest surface coverage which makes this reagent superior to the commonly used standard silylation reagent hexamethyldisilazane. This higher silylation efficiency of tetramethyldisilazane might have important implications for the tuning of the catalytic properties of heterogeneously acting catalysts. Sterically bulkier disilazane reagents such as tetraphenyldimethyldisilazane produce a surface morphology with a considerable number of uniformly distributed silanol sites left which, however, are accessible for further modification reactions. Both *consecutive* and *competitive* silylation reactions reveal important details of the kinetics of this silylation reaction and support a controlled surface functionalization as shown for vinyl moieties. These vinyl groups provide a unique platform for subsequent modification reactions as verified by the hydroboration reaction. Preliminary grafting experiments of catalytically relevant metalorganic species reveal that presilylation is an efficient tool to direct the number and uniform distribution of reactive surface species, while simultaneously increasing the hydrophobicity of the inorganic/organic hybrid material.

Acknowledgment. We thank the Deutsche Forschungsgemeinschaft (DFG) and Degussa-Hüls AG for financial support of this research. R.A. thanks the DFG for the award of a fellowship. M.W. thanks the Fonds der Chemischen Industrie (FCI) for a fellowship (with participation of the Bundesministerium für Bildung, Wissenschaft, Forschung und Technologie). G.E. acknowledges financial support by the FCI. Additionally, generous support from Prof. W. A. Herrmann and Prof. J. Weitkamp is gratefully acknowledged.

References and Notes

(1) For reviews, see: (a) Schüth, F. *Ber. Bunsen-Ges. Phys. Chem.* **1995**, *99*, 1306. (b) Sayari, A. *Chem. Mater.* **1996**, *8*, 1840. (c) Biz, S.; Occelli, M. L. *Catal. Rev.−Sci. Eng.* **1998**, *40*, 329.

(2) For an example, see: Oldroyd, R. D.; Sankar, G.; Thomas, J. M.; Özkaya, D. *J. Phys. Chem. B* **1998**, *102*, 1849.

(3) For recent reviews on the derivatization of mesoporous materials of the M41S family, see: (a) Moller, K.; Bein, T. *Chem. Mater.* **1998**, *10*, 2950. (b) Clark, J.; Macquarrie, D. J. *Chem. Commun.* **1998**, 853.

(4) For examples, see: (a) Burkett, S. L.; Sims, S. D.; Mann, S. *Chem. Commun.* **1996**, 1367. (b) Macquarrie, D. J. *Chem. Commun.* **1996**, 1961. (c) Lim, M. H.; Blanford, C. F.; Stein, A. *J. Am. Chem. Soc.* **1997**, *119*, 4090. (d) Fowler, C. E.; Burkett, S. L.; Mann, S. *Chem. Commun.* **1997**, 1769. (e) Macquarrie, D. J.; Jackson, D. B. *Chem. Commun.* **1997**, 1781. (f) Lim, M. H.; Blanford, C. F.; Stein, A. *Chem. Mater.* **1998**, *10*, 467. (g) Van Rhijn, W. M.; De Vos, D. E.; Sels, B. F.; Bossaert, W. D.; Jacobs, P. A. *Chem. Commun.* **1998**, 317. (h) Hall, S. R.; Fowler, C. E.; Lebeau, B.; Mann, S. *Chem. Commun.* **1999**, 201.

(5) For examples, see: (a) Tatsumi, T.; Koyano, K. A.; Igarashi, N. *Chem. Commun.* **1998**, 325. (b) Klein, S.; Maier, W. F. *Angew. Chem.* **1996**, *108*, 2376; *Angew. Chem., Int. Ed. Engl.* **1996**, *35*, 2230.

(6) Choplin, A. *J. Mol. Catal.* **1994**, *86*, 501.

(7) Vansant, E. F.; Van Der Voort, P.; Vrancken K. C. (Eds.), Characterization and Chemical Modification of the Silica Surface (*Stud. Surf. Sci. Catal.*, Volume 93), Elsevier: Amsterdam, 1995.

(8) For chlorosilane silylation of MCM-41 silicas, see: (a) Chen, J.; Li, Q.; Xu, R.; Xiao, F. *Angew. Chem.* **1995**, *107*, 2898; *Angew. Chem., Int. Ed. Engl.* **1995**, *34*, 2694. (b) Zhao, X. S.; Lu, G. Q.; Whittaker, A. K.; Millar, G. J.; Zhu, H. Y. *J. Phys. Chem.* **1997**, *101*, 6525. (c) Koyano, K. A.; Tatsumi, T.; Tanaka, Y.; Nakata, S. *J. Phys. Chem. B* **1997**, *101*, 9436. (d) Shephard, D. S.; Zhou, W.; Maschmeyer, T.; Matters, J. M.; Roper, C. L.; Parson, S.; Johnson, B. F. G.; Duer, M. J. *Angew. Chem.* **1998**, *110*, 2847; *Angew. Chem., Int. Ed. Engl.* **1998**, *37*, 2719.

(9) For alkoxysilane silylation of MCM-41 silicas, see: (a) Sutra, P.; Brunel, D. *Chem. Commun.* **1996**, 2485. (b) Díaz, J. F.; Balkus, K. J., Jr.; Bedioui, F.; Kurshev, V.; Kevan, L. *Chem. Mater.* **1997**, *9*, 61. (c) Rao, Y. V. S.; De Vos, D. E.; Bein, T.; Jacobs, P. A. *Chem. Commun.* **1997**, 355. (d) Liu, C.-J.; Li, S.-G.; Pang, W.-Q.; Che, C.-M. *Chem. Commun.* **1997**, 65. (e) Feng, X.; Fryxell, G. E.; Wang, L.-Q.; Kim, A. Y.; Liu, J.; Kemner, K. M. *Science* **1997**, *276*, 923. (f) Mercier, L.; Pinnavaia, T. J. *Adv. Mater.* **1997**, *9*, 500. (g) Subba Rao, Y. V.; De Vos, D. E.; Jacobs, P. A. *Angew. Chem.* **1997**, *109*, 2776; *Angew. Chem., Int. Ed. Engl.* **1997**, *36*, 2661. (h) Kantam, M. L.; Bandyopadhyay, T.; Rahman, A.; Reddy, N. M.; Choudary, B. M. *J. Mol. Catal. A* **1998**, *133*, 293.

(10) (a) Hertl, W.; Hair, M. L. *J. Phys. Chem.* **1971**, *75*, 2181. (b) Sindorf, D. W.; Maciel, G. E. *J. Phys. Chem.* **1982**, *86*, 5208.

(11) Anwander, R.; Palm, C.; Stelzer, J.; Groeger, O.; Engelhardt, G. *Stud. Surf. Sci. Catal.* **1998**, *117*, 135.

(12) Beck, J. S.; Vartuli, J. C.; Roth, W. J.; Leonowicz, M. E.; Kresge, C. T.; Schmitt, K. D.; Chu, C. T.-W.; Olson, D. H.; Sheppard, E. W.; McCullen, S. B.; Higgins, J. B.; Schlenker, J. L. *J. Am. Chem. Soc.* **1992**, *114*, 10834.

(13) Boger, T.; Roesky, R.; Gläser, R.; Ernst, S.; Eigenberger, G.; Weitkamp, J. *Microporous Mater.* **1997**, *8*, 79.

(14) (a) Ryoo, R.; Kim, J. M. *J. Chem. Soc., Chem. Commun.* **1995**, 711. (b) Voegtlin, A. C.; Matijasic, A.; Patarin, J.; Sauerland, C.; Grillet, Y.; Huve, L. *Microporous Mater.* **1997**, *10*, 137. (c) Edler, K. J.; White, J. W. *Chem. Mater.* **1997**, *9*, 1226.

(15) Schmidt, R.; Stöcker, M.; Hansen, E.; Akporiaye, D.; Ellestad, O. E. *Microporous Mater.* **1995**, *3*, 443.

(16) Ryoo, R.; Jun, S. *J. Phys. Chem.* **1997**, *101*, 317.

(17) (a) Schmidt, R.; Hansen, E. W.; Stöcker, M.; Akporiaye, D.; Ellestad, O. H. *J. Am. Chem. Soc.* **1995**, *117*, 4049. (b) Cheng, C.-F.; Park, D. H.; Klinowski, J. *J. Chem. Soc., Faraday Trans.* **1997**, *93*, 193.

(18) Sing, K. S. W.; Everett, D. H.; Haul, H. R. A. W.; Moscou, L.; Pierotti, R. A.; Rouquérol, J.; Siemieniewska, T. *Pure Appl. Chem.* **1985**, *57*, 603.

(19) Barret, E. P.; Joyner, L. G.; Halenda, P. P. *J. Am. Chem. Soc.* **1951**, *73*, 373.

(20) Snyder, L. R.; Ward, J. W. *J. Phys. Chem.* **1966**, *70*, 3941.

(21) (a) Cauvel, A.; Renard, G.; Brunel, D. *J. Org. Chem.* **1997**, *62*, 749. (b) D'Amore, M. B.; Schwarz, S. *Chem. Commun.* **1999**, 121.

(22) For examples, see: (a) Bohemen, J.; Langer, S. H.; Perrett, R. H.; Purnell, J. H. *J. Chem. Soc., London* **1960**, 2444. (b) Boudreau, S. P.; Cooper, W. T. *Anal. Chem.* **1989**, *61*, 41.

(23) Anwander, R.; Runte, O.; Eppinger, J.; Gerstberger, G.; Herdtweck, E.; Spiegler, M. *J. Chem. Soc., Dalton Trans.* **1998**, 847.

(24) Haukka, S.; Root, A. *J. Phys. Chem.* **1994**, *98*, 1695.

(25) Hua, D.-W.; Smith, D. M. *Langmuir* **1992**, *8*, 2753.

(26) Anwander, R.; Palm, C.; Groeger, O.; Engelhardt, G. *Organometallics* **1998**, *17*, 2027.

(27) Chronister, C. W.; Drago, R. S. *J. Am. Chem. Soc.* **1993**, *115*, 4793.

(28) For detailed FTIR investigations of mesoporous materials of the M41S family, see: (a) Ishikawa, T.; Matsuda, M.; Yasukawa, A.; Kandori, K.; Inagaki, S.; Fukushima, T.; Kondo, S. *J. Chem. Soc., Faraday Trans.* **1996**, *92*, 1985. (b) Jentys, A.; Pham, N. H.; Vinek, H. *J. Chem. Soc., Faraday Trans.* **1996**, *92*, 3287.

(29) Eppinger, J. Ph.D. Thesis, Technische Universität München, 1999.

(30) Jaroniec, C. P.; Kruk, M.; Jaroniec, M.; Sayari, A. *J. Phys. Chem. B* **1998**, *102*, 5503.

(31) Hayes, G. R.; Clague, A. D. H.; Huis, R.; van der Velden, G. *Appl. Surf. Sci.* **1982**, *10*, 247.

(32) (a) Huo, Q.; Margolese, D. I.; Ciesla, U.; Demuth, D. G.; Feng, P.; Gier, T. E.; Sieger, P.; Firouzi, A.; Chmelka, B. F.; Schüth, F.; Stucky, G. D. *Chem. Mater.* **1994**, *6*, 1176. (b) Firouzi, A.; Kumar, D.; Bull, L. M.; Besier, T.; Sieger, P.; Huo, Q.; Walker, S. A.; Zasadzinski, J. A.; Glinka, C.; Nicol, J.; Margolese, D.; Stucky, G. D.; Chmelka, B. F. *Science* **1995**, *267*, 1138.

(33) Ingall, M. D. K.; Honeyman, C. H.; Mercure, J. V.; Bianconi, P. A.; Kunz, R. R. *J. Am. Chem. Soc.* **1999**, *121*, 3607.
(34) For a recent review, see: Buriak, J. M. *Chem. Commun.* **1999**, 1051.
(35) Hay, J.; Porter, D.; Raval, H. *Chem. Commun.* **1999**, 81.
(36) Feher, F. J.; Soulivong, D.; Eklund, A. G.; Wyndham, K. D. *Chem. Commun.* **1997**, 1185.
(37) Soderquist, J. A.; Brown, H. C. *J. Org. Chem.* **1980**, *45*, 3571.
(38) Bonhomme, C.; Toledano, P.; Maquet, J.; Livage, J.; Bonhomme-Coury, L. *J. Chem. Soc., Dalton Trans.* **1997**, 1617.
(39) Morrow, B. A.; McFarlane, R. A. *Langmuir* **1986**, *2*, 315.
(40) For recent examples, see: (a) Alt, G. A. *J. Chem. Soc., Dalton Trans.* **1999**, 1703. (b) Suzuki, N.; Asami, H.; Nakamura, T.; Huhn, T.; Fukuoka, A.; Ichikawa, M.; Saburi, M.; Wakatsuki, Y. *Chem. Lett.* **1999**, 341 and references therein.
(41) For the immobilization of group 4b metallocene complexes on MCM-41, see: (a) Maschmeyer, T.; Rey, F.; Sankar, G.; Thomas, J. M. *Nature* **1995**, *378*, 159. (b) Ko, Y. S.; Han, T. K.; Park, J. W.; Woo, S. I. *Macromol. Rapid Commun.* **1996**, *17*, 749. (c) Tudor, J.; O'Hare, D. *Chem. Commun.* **1997**, 603. (d) Van Looveren, L. K.; Geysen, D. F. M. C.; Vercruysse, K. A. L.; Wouters, B. H. J.; Grobet, P. J.; Jacobs, P. A. *Angew. Chem., Int. Ed. Engl.* **1998**, *37*, 517.